PAPER

Check for updates

Zinc bromide: a general mediator for the ionothermal synthesis of microporous polymers *via* cyclotrimerization reactions†

Jaehwan Kim, ‡[a] Minh H. Le, ‡[a] Makayla C. Spicer,[a] Casandra M. Moisanu,[a] Suzi M. Pugh[b] and Phillip J. Milner ⋆[a]

Conjugated microporous polymers (CMPs) are porous organic materials that display (semi)conducting behavior due to their highly π-conjugated structures, making them promising next-generation materials for applications requiring both electrical conductivity and porosity. Currently, most CMPs and related porous aromatic frameworks (PAFs) are prepared using expensive transition metals (*e.g.*, Pd), significantly increasing the costs associated with their synthesis. Lewis acid-mediated cyclotrimerization reactions of methyl ketones and nitriles represent promising and green alternative methods for CMP and PAF synthesis. Herein, we demonstrate that the generality of the solvent-free cyclotrimerization reactions is significantly improved by using $ZnBr_2$ instead of $ZnCl_2$ as the ionothermal medium. Specifically, we show that 1,4-diacetylbenzene (**DAB**), 4,4′-diacetylbiphenyl (**DABP**), 2,7-diacetylfluorene (**DAF**), 1,3,5-triacetylbenzene (**TAB**), tetrakis(4-acetylphenyl)methane (**TAPM**), and 1,4-dicyanobenzene (**DCNB**) can be polymerized in molten $ZnBr_2$ to produce highly conjugated and microporous materials, as confirmed by 77 K N_2 adsorption measurements, IR, and solid-state NMR. These findings support that $ZnBr_2$ is an excellent Lewis acid mediator and medium for the ionothermal synthesis of porous organic materials.

[a]*Department of Chemistry and Chemical Biology, Cornell University, Ithaca, NY, 14850, USA. E-mail: pjm347@cornell.edu*

[b]*Yusuf Hamied Department of Chemistry, University of Cambridge, Cambridge, CB2 1EW, UK*

† Electronic supplementary information (ESI) available: Experimental and electrochemical data. See DOI: https://doi.org/10.1039/d3ta01471a

‡ These authors contributed equally.

Introduction

Conjugated microporous polymers (CMPs) are intriguing amorphous organic materials that blend the porosity of porous organic polymers (POPs) with the extended π-conjugation of 2-dimensional materials.[1–3] This combination makes them promising for applications that require guest-accessible pores in a (semi)conducting platform, such as heterogeneous electro/photocatalysis and supercapacitive charge storage.[4,5] Relatedly, porous aromatic frameworks (PAFs) are ultra-stable, 3-dimensional POPs that are valuable for heterogeneous catalysis, toxic gas capture, and water purification.[6] Both CMPs and PAFs are typically prepared under solvothermal conditions using Pd- or Ni-mediated reactions,[7,8] contributing greatly to their synthesis costs on scale. Residual metal species can also contaminate the final insoluble polymers and alter their catalytic activities in ways that are difficult to predict.[9,10] Although green approaches to preparing POPs have emerged in recent years,[11] there remains

an urgent need for general and sustainable methods amenable to the synthesis of CMPs and PAFs from simple monomers.

Recently, cyclotrimerization reactions of methyl ketones[12–29] and nitriles[30–32] have emerged as promising approaches to prepare CMPs and PAFs without expensive transition metal catalysts and, in many cases, without additional organic solvents. In particular, the acid-catalyzed synthesis of POPs from polyacetylated monomers proceeds through dimerization *via* the aldol reaction to produce α,β-unsaturated ketones, followed by cyclotrimerization to produce 1,3,5-substituted benzene rings.[20] Notably, only water is produced as a byproduct of this process, making it an attractive method for polymer synthesis.

With Brønsted acids such as methanesulfonic acid (MsOH) and *p*-toluenesulfonic acid (TsOH), the aldol reaction produces a mixture of α,β-unsaturated ketone and aromatic linkages due to incomplete cyclotrimerization, as evidenced by residual carbonyl (C=O) groups detected by infrared (IR) spectroscopy and tunneling electron microscopy (TEM).[13,14,18,19,25,26] These functionalities likely reduce the overall conjugation of the polymeric materials and change their fundamental optoelectronic properties as well.[18] On the other hand, ionothermal Lewis acid mediators such as $ZnCl_2$ drive cyclotrimerization reactions to higher conversions,[12] but the requisite harsh reaction conditions lead to significant degradation and carbonization of the resulting polymers.[33] As a result, this approach is

This journal is © The Royal Society of Chemistry 2023

J. Mater. Chem. A, 2023, **11**, 17159–17166 | **17159**

currently only suitable for synthesizing a single CMP from 1,3,5-triacetylbenzene (**TAB**), referred to herein as **TAB-CMP**; all other tested monomers yielded non-porous or low surface area materials.[12] The identification of superior Lewis acids that can function as both the mediator and reaction medium would enable a broader range of monomers to be converted into highly conjugated porous organic materials.

Herein, we demonstrate that simply switching the ionothermal solvent from $ZnCl_2$ to $ZnBr_2$ greatly extends the scope of monomers compatible with the synthesis of CMPs and PAFs *via* ionothermal aldol cyclotrimerization. Using $ZnBr_2$, five monomers could be effectively converted into microporous organic polymeric materials, with high conversion of the carbonyl groups into aromatic rings confirmed by Attenuated Total Reflectance IR spectroscopy (ATR-IR) and energy-dispersive X-ray spectroscopy (EDS). Notably, $ZnBr_2$ could also be used to prepare a porous covalent triazine framework (CTF) under ionothermal conditions. Together, these results indicate that $ZnBr_2$ is a potential replacement for $ZnCl_2$ with improved monomer compatibility, paving the way for the sustainable synthesis of other POPs under solvent-free conditions.

Results and discussion

$ZnBr_2$ as an alternative Lewis acid to $ZnCl_2$

Because $ZnCl_2$ is widely employed as a strong Lewis acid in both fine chemical and polymer synthesis,[34] we hypothesized that the poor scope observed for ionothermal aldol cyclotrimerization reactions with $ZnCl_2$ is likely due to its aggressive reactivity, which leads to significant monomer degradation and material carbonization.[12,33] As such, switching to a milder Lewis acid should improve the monomer compatibility of this reaction. Previous work has shown that $ZnBr_2$ enables delicate reactions that do not proceed well with stronger Lewis acids such as $TiCl_4$.[35,36] As an added benefit, switching from Cl^- counteranions ($\sim$1.75 Å) to larger Br^- counteranions ($\sim$1.85 Å) should help to better template forming micropores and prevent their collapse during the polymerization process.[37–39] As such, we surmised that $ZnBr_2$ might serve as a better ionothermal medium for POP synthesis. Indeed, our preliminary results using a molecular model system support that both $ZnCl_2$ and $ZnBr_2$ are competent mediators for aldol cyclotrimerization reactions under solvothermal conditions (ESI Section 5, Fig. S133–S135†).

The ability of $ZnBr_2$ to mediate POP synthesis from polyacetylated monomers was initially assessed using 1,4-diacetylbenzene (**DAB**) as a model monomer to produce a CMP termed **CORN-CMP-2** (CORN = Cornell University) and referred to herein as **DAB-CMP** (Fig. 1, ESI Section 4†). Previous work has shown that Brønsted acids, such as MsOH (*p*-PPN, PPN = porous polymer network),[14,19] TsOH (**OFC-1B**, OFC = porous organic framework by the cyclotrimerization reaction),[22,26] and *in situ* generated HCl (**OFC-1A**)[26] can be used to prepare porous polymeric materials from **DAB**. In contrast, the combination of **DAB** and $ZnCl_2$ under ionothermal conditions at 300 °C or 400 °C produces non-porous solids (ESI Table S20†).[12] Using a custom-built apparatus (ESI Fig. S7†), varying equivalents of
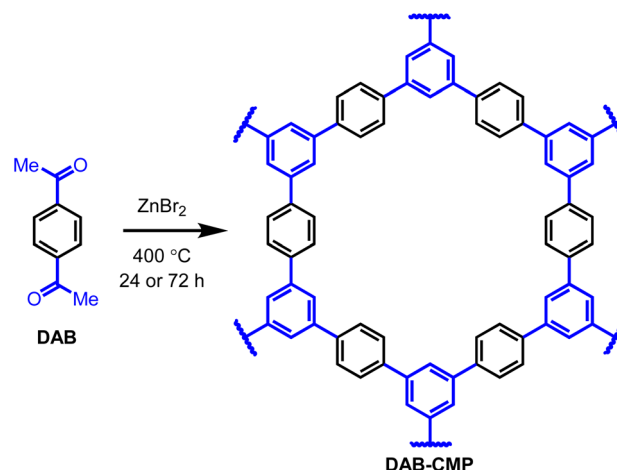

Fig. 1 Synthesis of **DAB-CMP** from **DAB** with varying equivalents of $ZnBr_2$ at 400 °C for either 24 or 72 h.

anhydrous $ZnBr_2$ (1.00 equiv., 5.00 equiv., and 10.0 equiv.) were combined with **DAB** under vacuum in flame-sealed tubes (see ESI Section 3† for details). The solid mixtures were transferred to a furnace and allowed to stand at 400 °C ($ZnBr_2$ melting point = 394 °C) for either 24 h or 72 h. After cooling to room temperature, the resulting black solids were rinsed with aqueous HCl and water to remove residual Zn^{2+} salts and then with tetrahydrofuran (THF) and acetone to remove soluble organic species. The solids were finally dried under vacuum at 120 °C overnight prior to characterization by ATR-IR, surface area analysis, and powder X-ray diffraction (PXRD) (Fig. 2). All prepared materials were found to be amorphous by PXRD (ESI Fig. S19 and S20†) and scanning electron microscopy (SEM, ESI Fig. S9†). It should be noted that the black color of these solids is likely due to partial graphitization, a common challenge associated with high-temperature ionothermal synthesis.[33] At this time, we cannot rule out that *in situ* generated HBr (resulting from the reaction of water produced from the polymerization with $ZnBr_2$) plays a role under these conditions.

In contrast to the results obtained with Brønsted acids,[19,22] only weak residual C=O stretches ($\sim$1690 cm^{-1}) were observed in the ATR-IR spectra of all **DAB-CMP** materials synthesized with $ZnBr_2$ (Fig. 2a). The ATR-IR spectra of the samples prepared for 24 h, particularly that made with just 1.00 equiv. of $ZnBr_2$, contain additional C=O stretches ($\sim$1698 cm^{-1}) that are absent from materials made for 72 h (ESI Fig. S17 and S18†), indicative of incomplete cyclotrimerization.[22] The ATR-IR spectra of samples prepared with 5.00 or 10.0 equiv. of $ZnBr_2$ for 24 h and 1.00 equiv. or 5.00 equiv. of $ZnBr_2$ for 72 h were similar and dominated by a large stretch near 1570 cm^{-1}, corresponding to the newly formed 1,3,5-substituted aromatic rings.[12,22] The corresponding aromatic stretch in **DAB** is present as a shoulder near 1600 cm^{-1} that is masked by the dominant carbonyl C=O stretch. Together, the ATR-IR spectra support that $ZnBr_2$ is a competent mediator for aldol cyclotrimerization reactions and that ionothermal conditions that are too gentle or too harsh lead to sub-optimal results.
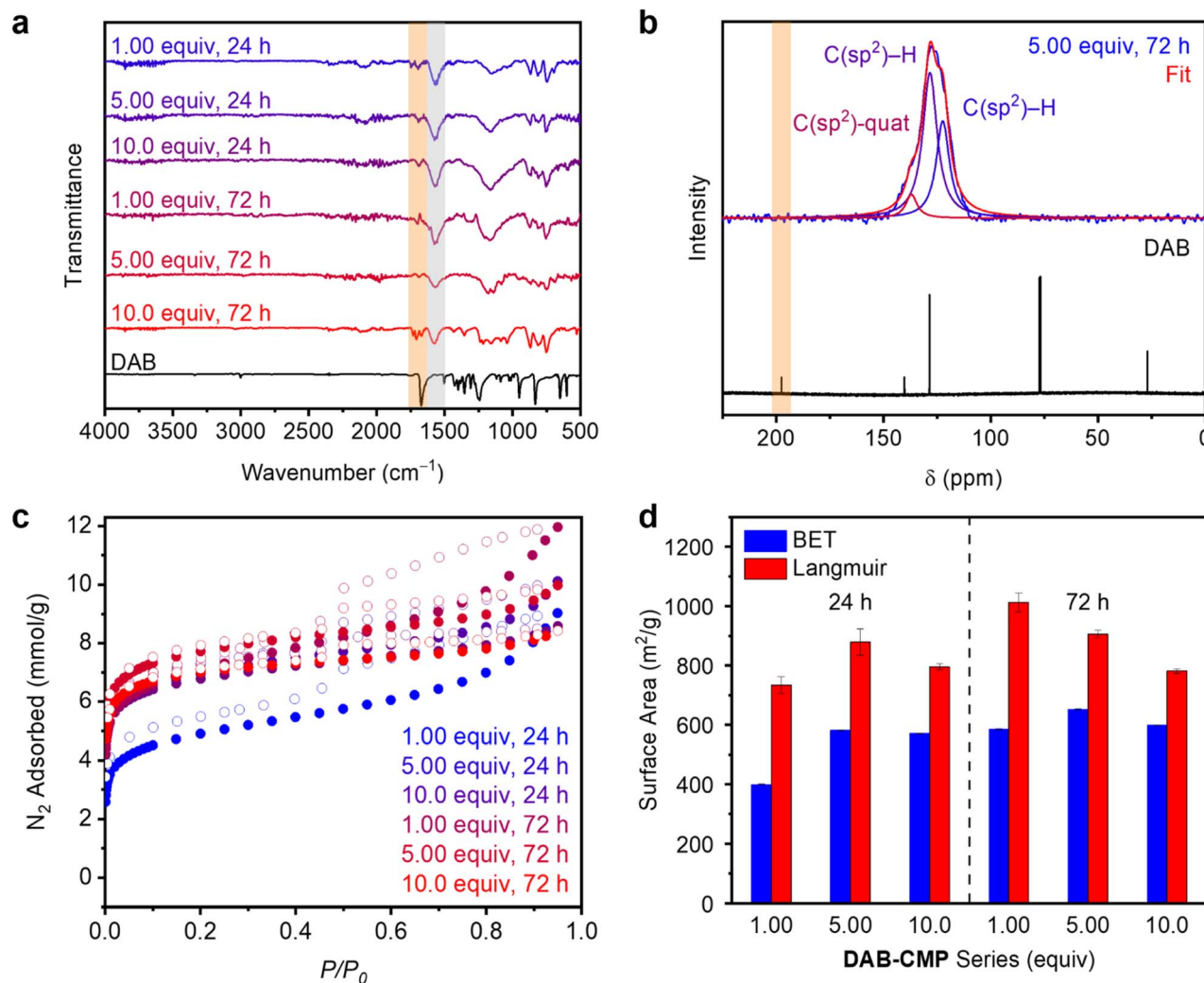
Fig. 2 Solid-state characterization of the **DAB-CMP** series made with various equivalents of ZnBr$_2$ at 400 °C for 72 h. (a) ATR-IR spectra of **DAB** and the **DAB-CMP** series. The orange highlighted region indicates the disappearance of the C≡O stretch from **DAB**, and the gray highlighted region indicates the appearance of a C≡C aromatic stretch in the polymeric materials. (b) CP MAS ^{13}C SSNMR (125 MHz) spectrum with fitting and deconvolution of **DAB-CMP**-5.00 equiv., 72 h and the solution state (125 MHz, CDCl$_3$) ^{13}C NMR of **DAB**, indicating the disappearance of a carbonyl peak at approximately δ 200 ppm. (c) 77 K N$_2$ adsorption (filled circles) and desorption (open circles) isotherms of the **DAB-CMP** series and (d) summary of the BET and Langmuir surface areas of the **DAB-CMP** series.

The porosity of prepared **DAB-CMP** samples was assessed using 77 K N$_2$ adsorption/desorption isotherms (Fig. 2c and d). All six samples were found to be microporous, confirming that ZnBr$_2$ enables the synthesis of much higher surface area materials than ZnCl$_2$.[12] The lowest Brunauer–Emmett–Teller (BET) surface areas were determined for **DAB-CMP** prepared with 1.00 equiv. of ZnBr$_2$ for 24 h (399 ± 1 m^2 g^{-1}). The BET surface areas of the other samples were found to lie in a narrow range ($\sim$600 m^2 g^{-1}), with the material prepared under intermediate conditions (**DAB-CMP**-5.00 equiv., 72 h) possessing the highest BET surface area (651 ± 2 m^2 g^{-1}) of all samples. The BET surface area of **DAB-CMP**-5.00 equiv., 72 h is slightly lower than those reported previously for the related materials **OFC-1B** (780–895 m^2 g^{-1})[22,26] and **p-PPN** (802–1054 m^2 g^{-1}),[14,19] which possess a higher degree of approximately linear α,β-unsaturated ketone linkages that should decrease the density of the

polymeric material. The density functional theory (DFT) calculated pore size distribution of **DAB-CMP**-5.00 equiv., 72 h assuming a carbon slit pore model revealed a maximum at 11.4 Å (ESI Fig. S35†), which is comparable to the pore diameter predicted for the idealized, non-interpenetrated structure ($\sim$12 Å, ESI Fig. S156†).[19] Though **DAB-CMP**-5.00 equiv., 72 h possesses the highest BET surface area of all **DAB-CMP** samples, it should be noted that high surface area material (584 m^2 g^{-1}) could be prepared using just 1.00 equiv. of ZnBr$_2$, which is unusual for ionothermal POP synthesis.[33] Last, the ionothermal synthesis of porous **DAB-CMP** was found to be reproducible (ESI Fig. S31†).

To support that ZnBr$_2$ is a competent mediator for CMP synthesis, **DAB-CMP**-5.00 equiv., 72 h was further characterized using cross-polarized (CP) magic angle spinning (MAS) solid-state nuclear magnetic resonance spectroscopy (SSNMR,

Fig. 2b, ESI Fig. S33 and S34†), Raman spectroscopy (ESI Fig. S37†), EDS (ESI Fig. S10 and Table S2†), combustion elemental analysis (ESI Table S3†), X-ray photoelectron spectroscopy (XPS, ESI Fig. S11–S16 and Table S4†), and diffuse reflectance UV-Vis spectroscopy (ESI Fig. S36†). The CP MAS ^{13}C SSNMR spectrum of **DAB-CMP**-5.00 equiv., 72 h revealed a complex resonance localized near 127 ppm, which could be deconvoluted into signals corresponding to two different types of ^{13}C(sp^2)–H centers and one quaternary ^{13}C(sp^2) center (Fig. 2b). This spectrum is similar to those previously reported for **DAB-CMP** analogs prepared using Brønsted acid mediators.[14,26] Notably, resonances corresponding to residual carbonyl groups (~200 ppm) were not observed. The MAS ^{1}H SSNMR of **DAB-CMP**-5.00 equiv., 72 h contained only a single broad resonance centered around 7 ppm, corresponding to aromatic C(sp^2)–^{1}H centers (ESI Fig. S33†). Consistent with the lack of residual carbonyl groups observed by ATR-IR and SSNMR spectroscopies, the EDS and XPS spectra of **DAB-CMP**-5.00 equiv., 72 h contained only trace O, along with small amounts of residual Zn, Cl, and Br (ESI Tables S2 and S4†). The presence of Cl in the washed and activated material is likely due to Br/Cl exchange with residual Zn salts upon soaking in HCl. Combustion elemental analysis (ESI Table S3†) confirmed the presence of trace Cl (1.55 wt%) in the sample, along with an observed H wt% (4.15%) close to the theoretical value (4.79%). Although Raman scattering lends evidence to some graphene-like character in the material, as expected of a highly conjugated material (ESI Fig. S37†), the detection of the expected amount of H in the sample supports that **DAB-CMP** was not completely carbonized under the ionothermal conditions. Last, the diffuse reflectance UV-Vis spectrum (ESI Fig. S36†) of **DAB-CMP** revealed broad absorbance over the visible regime, consistent with its black color and extended conjugated structure.[12,26] Overall, the spectroscopic and gas sorption data herein support the successful synthesis of microporous **DAB-CMP** using ZnBr$_2$ as an ionothermal mediator.

In order to assess whether ZnBr$_2$ really is the optimal ionothermal mediator for aldol cyclotrimerization reactions, we evaluated sixteen other Lewis acid mediators, focusing on low-melting (≤400 °C) Zn^{2+}, Sn^{2+}, Al^{3+}, Fe^{3+}, Bi^{3+}, Si^{4+}, Ti^{4+}, and Sb^{5+} salts (ESI Table S20, Section 6†). All Lewis acids were tested close to their melting point (or boiling point for salts that melt near room temperature) to minimize potential carbonization. The Lewis acids Al(NO$_3$)$_3$·9H$_2$O, SbCl$_5$, SiCl$_4$, Zn(NO$_3$)$_2$·6H$_2$O, and Zn(OAc)$_2$·2H$_2$O (48–250 °C) did not yield any isolable polymeric materials. Similar to the results obtained with ZnCl$_2$ at 300 °C or 400 °C, the Lewis acids AlBr$_3$, TiCl$_4$, BiCl$_3$, Zn(SO$_3$CF$_3$)$_2$, and SnCl$_2$, along with a 3 : 1 : 1 eutectic mixture of ZnCl$_2$: KCl : NaCl (100–310 °C), produced non-porous or low surface area materials, indicative of significant degradation. Only the Lewis acids AlCl$_3$ (345 ± 2 m^2 g^{-1}), FeCl$_3$ (302 ± 1 m^2 g^{-1}), FeBr$_3$ (280 ± 2 m^2 g^{-1}), and TiBr$_4$ (489 ± 7 m^2 g^{-1}) (200–310 °C) produced porous solids with BET surface areas close to ZnBr$_2$ (651 m^2 g^{-1}), although the sample prepared using TiBr$_4$ was contaminated with residual crystalline TiO$_2$ (ESI Fig. S139†).[40,41] Ten low-melting potential Brønsted acids were also investigated (ESI Table S21, Section 6†), but only TsOH led
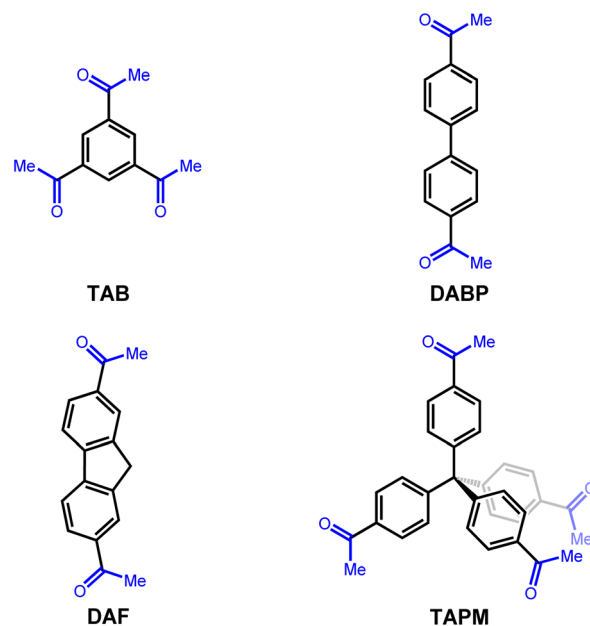

Fig. 3 Scope of monomers for POP synthesis *via* ZnBr$_2$-mediated aldol cyclotrimerization.

to high-surface area **DAB-CMP**, consistent with previous reports.[22,26] Together, these results support that ZnBr$_2$ is the optimal Lewis acid for POP synthesis *via* aldol cyclotrimerization.

Cyclotrimerization monomer scope using ZnBr$_2$

Given that ZnBr$_2$ enables ionothermal polymerization with at least one monomer (**DAB**) that does not work with ZnCl$_2$, its generality for POP synthesis was next examined using the monomers 1,3,5-triacetylbenzene (**TAB**), 4,4′-diacetylbiphenyl (**DABP**), 2,7-diacetylfluorene (**DAF**), and tetrakis(4-acetylphenyl) methane (**TAPM**) (Fig. 3). Among these, (porous) polymeric materials have been previously prepared from **TAB**,[12,14,18] **DABP**,[18,22,23,26] and **TAPM**,[25] whereas **DAF** represents a new monomer for this approach. As such, the optimal conditions for synthesizing **DAB-CMP** (5.00 equiv. ZnBr$_2$, 400 °C, 72 h) were employed to prepare materials referred to herein as **TAB-CMP** (**CORN-CMP-1**), **DABP-CMP** (**CORN-CMP-3**), **DAF-CMP** (**CORN-CMP-4**), and **TAPM-PAF** (**CORN-PAF-1**) (see ESI Section 4† for synthetic details). In all cases, black amorphous polymeric materials were obtained in good yields (>90%).

The four prepared materials were analyzed using the same techniques employed to characterize **DAB-CMP**-5.00 equiv., 72 h, including ATR-IR and CP MAS ^{13}C SSNMR spectroscopies, 77 K N$_2$ adsorption/desorption isotherms, EDS, and combustion analysis (Fig. 4, see ESI Section 4† for details). Consistent with the results obtained for **DAB-CMP** (Fig. 2a), ATR-IR spectroscopy confirmed the significant conversion of the carbonyl groups in the monomers (~1665–1685 cm^{-1}) into 1,3,5-substituted aromatic rings (~1565 cm^{-1}) in the polymeric materials in all cases (Fig. 4a; ESI Fig. S51, S69, S87, S105†). Consistently, the O wt% determined by EDS for **DABP-CMP**
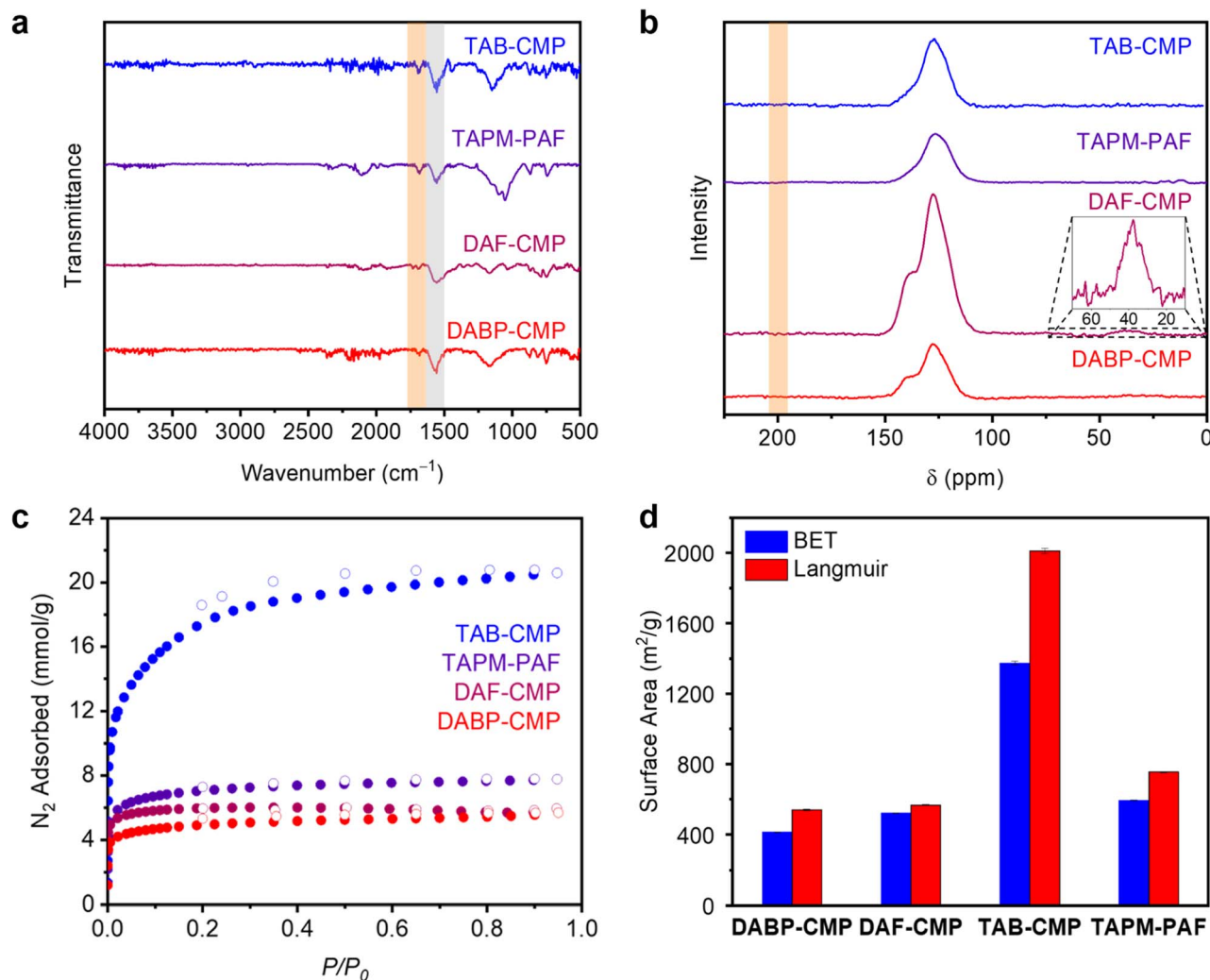
Fig. 4 Solid-state characterization of **DABP-CMP**, **DAF-CMP**, **DAF-CMP**, and **TAPM-PAF** made with 5.00 equiv. of ZnBr$_2$ at 400 °C for 72 h. (a) ATR-IR spectra of the polymers. The orange highlighted region shows the disappearance of C=O stretches from the respective monomers, and the gray highlighted region indicates the appearance of C=C aromatic stretches in the polymeric materials. (b) CP MAS ^{13}C SSNMR (125 MHz) spectra of the polymers. The orange highlighted region indicates the disappearance of a carbonyl peak at approximately δ 200 ppm from each of the respective monomers. (c) 77 K N$_2$ adsorption (filled circles) and desorption (open circles) isotherms of the polymers and (d) summary of the BET and Langmuir surface areas of the synthesized polymers.

(2.54%, ESI Fig. S42 and Table S5†), **DAF-CMP** (2.18%, ESI Fig. S60 and Table S8†), **TAB-CMP** (1.76%, ESI Fig. S78 and Table S11†), and **TAPM-PAF** (2.25%, ESI Fig. S96 and Table S14†) are all low. All prepared materials also contained only trace amounts of Zn, Cl, and Br by EDS and XPS, supporting that washing with aqueous HCl and water is sufficient to remove the vast majority of residual Zn salts. Furthermore, across all four materials, CP MAS ^{13}C SSNMR confirms the disappearance of the carbonyl groups and the appearance of chemical shifts at 125–130 ppm that correspond to aromatic carbons (Fig. 4b, ESI Fig. S50, S68, S86, and S104†). Notably, **DAF-CMP** retains a peak at 38.1 ppm, which corresponds to the sp^3-hybridized methylene carbons (–CH$_2$–) in the fluorene group (inset of Fig. 4b, ESI Fig. S68†). Unfortunately, the quaternary ^{13}C resonance expected for **TAPM-PAF** (around 70 ppm) could not be observed, likely due to its inherently weak nature and partial graphitization reducing its relative intensity (ESI Fig. S104†).[12]

The porosity of all four polymeric materials was also assessed using 77 K N$_2$ adsorption/desorption isotherms (Fig. 4c and d). Compared to samples of **DABP-CMP** prepared using Brønsted acid mediators, which display a broad range of BET surface areas (12–451 m^2 g^{-1}),[22,23,25] **DABP-CMP** has a relatively high surface area (415 ± 2 m^2 g^{-1}). The lower surface area of **DABP-CMP** compared to **DAB-CMP** – despite a nominally larger theoretical pore diameter (ESI Fig. S157 and 158†) – is likely due to interpenetration.[19,22,26] Similarly, the BET surface area of the new material **DAF-CMP** (522 ± 2 m^2 g^{-1}) is slightly lower than that of **DAB-CMP**. The BET surface area of **TAB-CMP** (1373 ± 11 m^2 g^{-1}) is higher than that reported using ZnCl$_2$ (929 ± 6 m^2 g^{-1})[12] and comparable to that for the optimal material prepared using MsOH (1235 m^2 g^{-1}),[14] reflecting its good quality. The surface area of this material is consistently higher than those of other cyclotrimerized microporous polymers, which is likely due to a lack of interpenetration and its defective,

This journal is © The Royal Society of Chemistry 2023

J. Mater. Chem. A, 2023, **11**, 17159–17166 | **17163**

non-planar structure (ESI Fig. S161†).[14] Last, the BET surface area determined for **TAPM-PAF** (594 ± 3 m² g⁻¹) is only slightly lower than that reported for the material prepared using thionyl chloride as a mediator (832 m² g⁻¹).[25] Critically, this surface area is much higher than that obtained using $ZnCl_2$ under similar conditions (133 ± 1 m² g⁻¹),[12] further reflecting the superiority of $ZnBr_2$ as an ionothermal mediator. Combined with the spectroscopic results outlined above, these surface area data confirm that $ZnBr_2$ is a general mediator for the ionothermal synthesis of porous materials *via* the aldol cyclotrimerization reaction.

Covalent triazine framework synthesis using $ZnBr_2$

Beyond the aldol reaction, the Lewis acid-catalyzed conversion of nitrile groups into 1,3,5-triazines is a general strategy for preparing covalent triazine frameworks (CTFs), which can either be crystalline (C) or amorphous (A).[30–32] Under ionothermal conditions, $ZnCl_2$ mediates the cyclotrimerization of 1,4-dicyanobenzene (**DCNB**) into CTF-1, referred to herein as **DCNB-CTF-A** (amorphous) or **DCNB-CTF-C** (crystalline) (Fig. 5).[32] Given the excellent performance of $ZnBr_2$ as an ionothermal mediator, we hypothesized that it could serve as a replacement for $ZnCl_2$ to enable the facile synthesis of CTFs as well. As such, we evaluated whether the combination of **DCNB** and $ZnBr_2$ (5.00 equiv. $ZnBr_2$, 400 °C, 40 h, time and temperature taken directly from literature for comparison[32]) can be used to prepare high-quality **DCNB-CTF**. After soaking in organic solvent and drying under vacuum, a shiny black solid was obtained in a good yield (90%, see ESI Section 4† for details). PXRD (ESI Fig. S125†) and SEM (ESI Fig. S113†) confirmed that the obtained material was amorphous, and thus it was assigned as **DCNB-CTF-A**.

DCNB-CTF-A was characterized by ATR-IR and CP MAS ¹³C SSNMR spectroscopies, 77 K N_2 adsorption/desorption, EDS, XPS, and combustion analysis (Fig. 6, see ESI Section 4† for details). ATR-IR confirmed the complete loss of the nitrile C≡N stretch in **DCNB** (2231 cm⁻¹) and the appearance of triazine rings in the polymerized material (1170 and 1590 cm⁻¹).[32] Notably, the ¹³C SSNMR spectrum of **DCNB-CTF-A** is comparable to those reported for CTFs synthesized with $ZnCl_2$ (ESI Fig. S123†),[42,43] and the XPS spectrum of **DCNB-CTF-A** shows a noticeably broadened C 1s signal, which could be deconvoluted into carbons in a triazine environment (N–C=N) and benzene environment (C–C=C) (Fig. S116†). The porosity of **DCNB-CTF-A** was assessed using 77 K N_2 adsorption/desorption measurements. Its BET surface area was determined to be 1446 ± 10 m² g⁻¹, which compares favorably to the reported surface areas for this material prepared at 400 °C with $ZnCl_2$ (920–1123 m² g⁻¹).[32,44] The DFT-calculated pore size distribution of **DCNB-CTF-A** assuming a carbon slit pore model also revealed
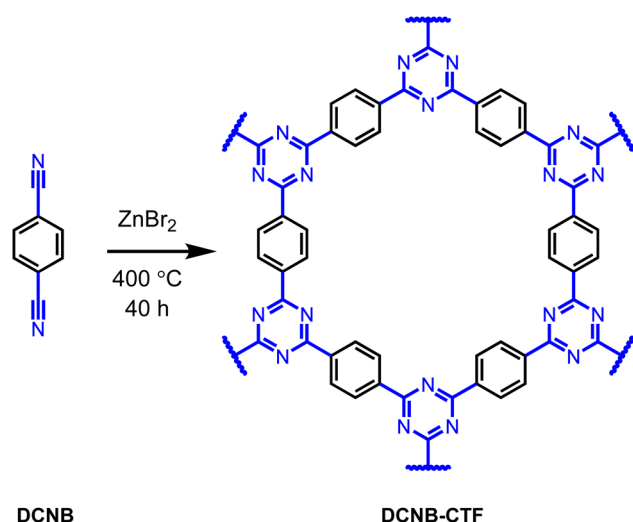

Fig. 5 Synthesis of **DCNB-CTF** from **DCNB** with 5.00 equiv. of $ZnBr_2$ at 400 °C for 40 h.
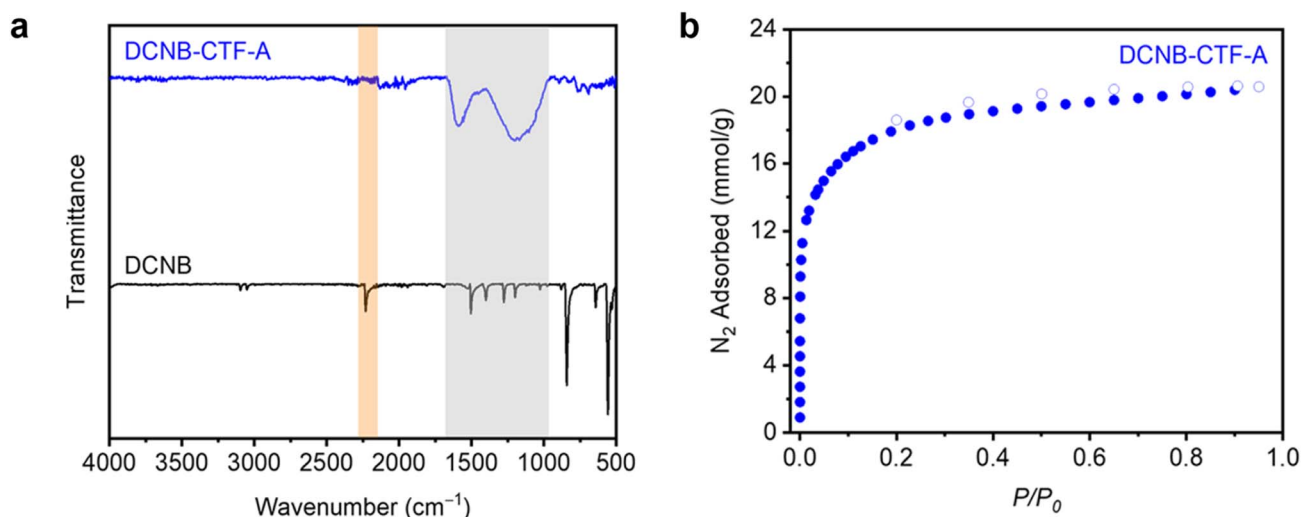

Fig. 6 Solid-state characterization of **DCNB-CTF-A** made with 5.00 equiv. of $ZnBr_2$ at 400 °C for 40 h. (a) ATR-IR spectra of **DCNB** and **DCNB-CTF-A**. The orange highlighted region shows the disappearance of the C≡N stretch from **DCNB**, and the gray highlighted region indicates the appearance of triazine stretches in **DCNB-CTF-A**. (b) 77 K N_2 adsorption (filled circles) and desorption (open circles) isotherms of **DCNB-CTF-A**.

17164 | *J. Mater. Chem. A*, 2023, **11**, 17159–17166

This journal is © The Royal Society of Chemistry 2023

a maximum at 11.4 Å (ESI Fig. S127†), similar to the pore diameter predicted for the idealized, non-interpenetrated structure (∼11 Å, ESI Fig. S165†). Notably, the synthesized **DCNB-CTF-A** did not contain detectable amounts of residual Zn or Br by EDS or XPS and contained only trace Cl (0.28 and 0.66 wt%, respectively). The observed C : N ratio from combustion analysis (5.7 : 1) is also comparable to those reported in the literature for samples prepared with $ZnCl_2$ (3.8 : 1–5.1 : 1).[32,44] These values are all higher than the theoretical value (3.4 : 1), indicating that some graphitization occurs with both ionothermal mediators.[33] Nonetheless, the data included here support the successful ionothermal synthesis of **DCNB-CTF-A** using $ZnBr_2$.

Conclusions

Herein, we have demonstrated that $ZnBr_2$ is a general ionothermal mediator for synthesizing a range of microporous polymers *via* cyclotrimerization reactions. Six materials could be prepared from simple methyl ketone or nitrile monomers under identical solvent-free conditions. An evaluation of twenty-five other Brønsted and Lewis acid mediators supports the exceptional performance of $ZnBr_2$. Our findings extend the scope of cyclotrimerized CMPs and PAFs that can be sustainably prepared, paving the way for their application as next-generation microporous materials for myriad applications. We hypothesize that $ZnBr_2$ may serve as a viable alternative to $ZnCl_2$ as an ionothermal mediator for the synthesis of other polymeric materials as well. Future work will focus on elucidating the mechanism of this ionothermal method, particularly on the potential role of *in situ* generated HBr.

Conflicts of interest

There are no conflicts to declare.

Acknowledgements

Notes and references

1 J.-S. M. Lee and A. I. Cooper, *Chem. Rev.*, 2020, **120**(4), 2171–2214.

2 S. Das, P. Heasman, T. Ben and S. Qiu, *Chem. Rev.*, 2017, **117**, 1515–1563.

3 N. Chaoui, M. Trunk, R. Dawson, J. Schmidt and A. Thomas, *Chem. Soc. Rev.*, 2017, **46**, 3302–3321.

4 K. Amin, N. Ashraf, L. Mao, C. F. J. Faul and Z. Wei, *Nano Energy*, 2021, **85**, 105958.

5 T. Zhang, G. Xing, W. Chen and L. Chen, *Mater. Chem. Front.*, 2020, **4**, 332–353.

6 Y. Tian and G. Zhu, *Chem. Rev.*, 2020, **120**, 8934–8986.

7 T. Ben, H. Ren, S. Ma, D. Cao, J. Lan, X. Jing, W. Wang, J. Xu, F. Deng, J. M. Simmons, S. Qiu and G. Zhu, *Angew. Chem., Int. Ed.*, 2009, **48**, 9457–9460.

8 J.-X. Jiang, F. Su, A. Trewin, C. D. Wood, N. L. Campbell, H. Niu, C. Dickinson, A. Y. Ganin, M. J. Rosseinsky, Y. Z. Khimyak and A. I. Cooper, *Angew. Chem., Int. Ed.*, 2007, **46**, 8574–8578.

9 J. Kosco, M. Sachs, R. Godin, M. Kirkus, L. Francas, M. Bidwell, M. Qureshi, D. Anjum, J. R. Durrant and I. McCulloch, *Adv. Energy Mater.*, 2018, **8**, 1802181.

10 F. C. Krebs, R. B. Nyberg and M. Jørgensen, *Chem. Mater.*, 2004, **16**, 1313–1318.

11 T. L. Church, A. B. Jasso-Salcedo, F. Björnerbäck and N. Hedin, *Sci. China: Chem.*, 2017, **60**, 1033–1055.

12 J. Kim, C. M. Moisanu, C. N. Gannett, A. Halder, J. J. Fuentes-Rivera, S. H. Majer, K. M. Lancaster, A. C. Forse, H. D. Abruña and P. J. Milner, *Chem. Mater.*, 2021, **33**, 8334–8342.

13 S. Che, C. Li, C. Wang, W. Zaheer, X. Ji, B. Phillips, G. Gurbandurdyyev, J. Glynn, Z.-H. Guo, M. Al-Hashimi, H.-C. Zhou, S. Banerjee and L. Fang, *Chem. Sci.*, 2021, **12**, 8438–8444.

14 C. Wang, C. Li, E. R. C. Rutledge, S. Che, J. Lee, A. J. Kalin, C. Zhang, H.-C. Zhou, Z.-H. Guo and L. Fang, *J. Mater. Chem. A*, 2020, **8**, 15891–15899.

15 C. Sreenivasulu, D. A. Thadathil, S. Pal and S. Gedu, *Synth. Commun.*, 2020, **50**, 112–122.

16 M.-Y. Wang, Q.-J. Zhang, Q.-Q. Shen, Q.-Y. Li and S.-J. Ren, *Chin. J. Polym. Sci.*, 2020, **38**, 151–157.

17 X. Yang and R. C. Smith, *J. Polym. Sci. Part A: Polym. Chem.*, 2019, **57**, 598–604.

18 S.-M. Jung, J. Park, D. Shin, H. Y. Jeong, D. Lee, I.-Y. Jeon, H. Cho, N. Park, J.-W. Yoo and J.-B. Baek, *Angew. Chem., Int. Ed.*, 2019, **58**, 11670–11675.

19 Z.-H. Guo, C. Wang, Q. Zhang, S. Che, H.-C. Zhou and L. Fang, *Mater. Chem. Front.*, 2018, **2**, 396–401.

20 B. Yang, J. Björk, H. Lin, X. Zhang, H. Zhang, Y. Li, J. Fan, Q. Li and L. Chi, *J. Am. Chem. Soc.*, 2015, **137**, 4904–4907.

21 S. K. Samanta, E. Preis, C. W. Lehmann, R. Goddard, S. Bag, P. K. Maiti, G. Brunklaus and U. Scherf, *Chem. Commun.*, 2015, **51**, 9046–9049.

22 F. M. Wisser, K. Eckhardt, D. Wisser, W. Böhlmann, J. Grothe, E. Brunner and S. Kaskel, *Macromol*, 2014, **47**, 4210–4216.

This journal is © The Royal Society of Chemistry 2023

J. Mater. Chem. A, 2023, **11**, 17159–17166 | **17165**

23 X. Zhu, C. Tian, S. Chai, K. Nelson, K. S. Han, E. W. Hagaman, G. M. Veith, S. M. Mahurin, H. Liu and S. Dai, *Adv. Mater.*, 2013, **25**, 4152–4158.

24 T. İslamoğlu, M. Gulam Rabbani and H. M. El-Kaderi, *J. Mater. Chem. A*, 2013, **1**, 10259.

25 Y.-C. Zhao, D. Zhou, Q. Chen, X.-J. Zhang, N. Bian, A.-D. Qi and B.-H. Han, *Macromol*, 2011, **44**, 6382–6388.

26 M. Rose, N. Klein, I. Senkovska, C. Schrage, P. Wollmann, W. Böhlmann, B. Böhringer, S. Fichtner and S. Kaskel, *J. Mater. Chem.*, 2011, **21**, 711–716.

27 R. S. Sprick, A. Thomas and U. Scherf, *Polym. Chem.*, 2010, **1**, 283–285.

28 Y. Shin, C. Wang, M. Englehard and G. E. Fryxell, *Microporous Mesoporous Mater.*, 2009, **123**, 345–348.

29 X.-Y. Cao, X.-H. Liu, X.-H. Zhou, Y. Zhang, Y. Jiang, Y. Cao, Y.-X. Cui and J. Pei, *J. Org. Chem.*, 2004, **69**, 6050–6058.

30 C. Krishnaraj, H. S. Jena, K. Leus and P. Van Der Voort, *Green Chem.*, 2020, **22**, 1038–1071.

31 M. Liu, L. Guo, S. Jin and B. Tan, *J. Mater. Chem. A*, 2019, **7**, 5153–5172.

32 P. Kuhn, M. Antonietti and A. Thomas, *Angew. Chem., Int. Ed.*, 2008, **47**, 3450–3453.

33 K. Wang, L.-M. Yang, X. Wang, L. Guo, G. Cheng, C. Zhang, S. Jin, B. Tan and A. Cooper, *Angew. Chem., Int. Ed.*, 2017, **56**, 14149–14153.

34 D. M. M. Rohe and H. U. Wolf, in *Ullmann's Encyclopedia of Industrial Chemistry*, ed., Wiley-VCH Verlag GmbH & Co. KGaA, Wiley-VCH Verlag GmbH & Co. KGaA, Weinheim, Germany, 2000, pp. 747–752.

35 P. Erdmann and L. Greb, *Angew. Chem., Int. Ed.*, 2022, **61**, e202114550.

36 I. Paterson, *Tetrahedron Lett.*, 1979, **20**, 1519–1520.

37 N. Fechler, T.-P. Fellinger and M. Antonietti, *Adv. Mater.*, 2013, **25**, 75–79.

38 J. S. Lee, X. Wang, H. Luo and S. Dai, *Adv. Mater.*, 2010, **22**, 1004–1007.

39 J. S. Lee, X. Wang, H. Luo, G. A. Baker and S. Dai, *J. Am. Chem. Soc.*, 2009, **131**, 4596–4597.

40 Ž. Antić, R. M. Krsmanović, M. G. Nikolić, M. Marinović-Cincović, M. Mitrić, S. Polizzi and M. D. Dramićanin, *Mater. Chem. Phys.*, 2012, **135**, 1064–1069.

41 H. Ijadpanah-Saravi, S. Dehestaniathar, A. Khodadadi-Darban, M. Zolfaghari and S. Saeedzadeh, *Desalin. Water Treat.*, 2016, **57**, 20503–20510.

42 V. M. Rangaraj, K. S. K. Reddy and G. N. Karanikolos, *Chem. Eng. J.*, 2022, **429**, 132160.

43 J. Jia, Z. Chen, Y. Belmabkhout, K. Adil, P. M. Bhatt, V. A. Solovyeva, O. Shekhah and M. Eddaoudi, *J. Mater. Chem. A*, 2018, **6**, 15564–15568.

44 P. Kuhn, A. Forget, D. Su, A. Thomas and M. Antonietti, *J. Am. Chem. Soc.*, 2008, **130**, 13333–13337.